

A detailed single chain model for molten poly(tetrafluoroethylene) from a novel structure refinement technique on neutron scattering data

B. Rosi-Schwartz* and G. R. Mitchell

Polymer Science Centre, J.J. Thomson Physical Laboratory, University of Reading, Reading RG6 2AF, UK

(Received 27 August 1993; revised 21 December 1993)

We present a new methodology that couples neutron diffraction experiments over a wide Q range with single chain modelling in order to explore, in a quantitative manner, the intrachain organization of non-crystalline polymers. The technique is based on the assignment of parameters describing the chemical, geometric and conformational characteristics of the polymeric chain, and on the variation of these parameters to minimize the difference between the predicted and experimental diffraction patterns. The method is successfully applied to the study of molten poly(tetrafluoroethylene) at two different temperatures, and provides unambiguous information on the configuration of the chain and its degree of flexibility. From analysis of the experimental data a model is derived with C–C and C–F bond lengths of 1.58 and 1.36 Å, respectively, a backbone valence angle of 110° and a torsional angle distribution which is characterized by four isometric states, namely a split *trans* state at $\pm 18^\circ$, giving rise to a helical chain conformation, and two *gauche* states at $\pm 112^\circ$. The probability of *trans* conformers is 0.86 at $T=350^\circ\text{C}$, which decreases slightly to 0.84 at $T=400^\circ\text{C}$. Correspondingly, the chain segments are characterized by long all-*trans* sequences with random changes in sign, rather anisotropic in nature, which give rise to a rather stiff chain. We compare the results of this quantitative analysis of the experimental scattering data with the theoretical predictions of both force fields and molecular orbital conformation energy calculations.

(Keywords: poly(tetrafluoroethylene); neutron scattering; structure refinement)

INTRODUCTION

The organization of non-crystalline polymeric materials at a local level is still unclear in many respects, even for polymers characterized by a relatively simple chemical composition, such as poly(tetrafluoroethylene) (PTFE). The determination of their local structure on a spatial scale between a few and 100 Å in terms of the configuration and conformation of the polymeric chain and of the packing characteristics of the chains in the bulk material represents a challenging problem, especially in view of the fact that many of the properties that are technologically relevant ultimately depend on the type and level of structural correlations on the microscopic scale.

Wide-angle diffraction techniques represent the most direct experimental tools to address such issues. Indeed, the sensitivity of these techniques, in particular wide-angle X-ray scattering (WAXS), to the details of the local correlations in amorphous macromolecules, has now been shown on a wide variety of polymeric systems^{1,2}.

In recent years the amount and detail of information obtainable from diffraction techniques has been extended with the development of neutron diffractometers operating on pulsed sources. Besides the typical advantages that neutrons offer, such as their high penetration and their

capability of investigating the structure directly, the availability of pulsed neutrons has opened up the possibility of exploring structural features over a very large region in reciprocal space ($Q_{\text{max}} \sim 100 \text{ \AA}^{-1}$), and therefore with a high spatial resolution which is certainly higher than that obtained by the more traditional X-ray based approach.

However, the recent literature remains sparse with regard to detailed wide-angle diffraction studies on the local structure of non-crystalline polymers, presumably due to the inherent difficulty in isolating and identifying the large number of correlations present in a diffraction pattern of such complex systems. In the case of WAXS investigations, the most successful data analysis strategy proposed to overcome these difficulties consists in the separation of the whole range of local structural correlations within a chain molecule in two types of contributions, i.e. those arising from correlations within the chain (intrachain) and those generated by correlations among different chains (interchain)¹.

While the interchain correlations give information on the nature and the type of packing in the bulk system, the intrachain contributions describe both the type of conformation and the extent of intrachain correlations. These can be extracted from experimental data at values of the momentum transfer $Q > 2 \text{ \AA}^{-1}$, by comparing the experimental scattering function and the ones

*To whom correspondence should be addressed

predicted by statistical models for the individual chains. These models are built by specifying the nature of the repeat unit and by assigning a set of possible rotational isomers to describe the internal chain rotations and their corresponding conditional probabilities of occurrence, consistently with the rotational isomeric state (RIS) theory^{3,4}.

The conformational characteristics of the individual polymer chains are fundamental in determining many of the useful physical properties of the material. The detailed study of conformational correlations is therefore of great interest. PTFE is a very interesting material to study from this point of view, in that little is known at its intrachain structure at a quantitative level, despite the wide technological exploitation of its unique properties of stiffness⁵.

The chemical structure of the PTFE chain is considered one of the simplest, with the repeat unit being analogous to that of polyethylene. The stiffness of PTFE can be explained by the characteristics of the individual chains. The van der Waals radius of the fluorine atom is considerably larger than that of the hydrogen atom. As a consequence, the van der Waals interactions between non-bonded atoms are more repulsive in PTFE than in polyethylene. These differences in intramolecular interactions result in profound differences in the configurational characteristics of the two systems. The PTFE molecule adopts a helical configuration in the crystalline state⁶, whereas polyethylene assumes a planar all-*trans* form⁷. The steric repulsions between non-bonded fluorine atoms are also responsible for the potential barrier to rotation in hexafluoroethane (4.35 kcal) being considerably higher than that for ethane (3.29 kcal)⁸. This is therefore the reason that the PTFE chain is less flexible than the polyethylene one. Indications of this reduced flexibility are the very high melting point (600 K) and the high melt viscosity of PTFE. A high level of chain stiffness was also supported by a detailed study of the chain configuration through the analysis of experimental dipole moments of perfluoroalkane molecules at room temperature⁹ and by a predictive calculation of the PTFE persistence length¹⁰.

While a relevant number of theoretical models and predictions of the single chain conformation of PTFE, mainly in the crystalline form, but also in the molten state, can be found in the literature, experimental investigations in the melt are scarce. Traditionally, the chain conformation and configuration of polymeric systems have been investigated by small-angle scattering techniques, mainly small-angle neutron scattering, which exploits isotopic substitution (mainly deuteration) to achieve different levels of contrast in the scattering signal, thus yielding the desired structural information. PTFE is not amenable to such a study, due to the fact that it does not contain hydrogen, and the isotopic substitution method does not work. After an initial, rather cursory X-ray scattering investigation by Kilian and Jenckel¹¹, a later and more detailed WAXS study was carried out^{12,13}. The picture drawn from that latter work was that of a highly persistent chain, characterized by a probability of *trans* torsions $p_t > 0.8$ and a high level of anisotropy in orientational segmental correlations. However, the agreement between model and experiment was not completely satisfactory.

This contribution is part of a larger programme, in which we have been involved in recent years, aimed at exploiting neutrons as a probe of local structure in

amorphous polymeric materials. In this work, we focus attention on the extraction of detailed quantitative information on the single chain properties of molten PTFE from its neutron diffraction pattern, taking advantage of the extended Q region explored by this experiment. We present a new method that quantitatively compares single chain stochastic models of the PTFE molecule and their predicted diffraction pattern with the one that has been obtained experimentally. We show the sensitivity of this approach to the different structural parameters and we explore the role of the various conformational parameters in the diffraction pattern. The values obtained for the geometric parameters will be discussed in the light of semiempirical quantum mechanical orbital calculations that were performed on the same material. Finally, this method allows us to draw, for the first time, a detailed description of the particular single chain properties of PTFE.

A preliminary qualitative report of the technique has been presented elsewhere¹⁴.

MODELLING TECHNIQUE

The single chain atomistic models were built, and the scattering curves calculated, by using an in-house modelling program, running on an Amdhal mainframe¹⁵.

The major problem of simulating a polymer chain, thereby describing its conformational correlations, arises because of the internal rotations in molecules, with the rotations about the skeletal bonds being particularly important. It is well established¹⁶ that conformational arrangements exist which are separated by energy barriers, thus giving rise to conformational transitions.

The description is greatly simplified by adopting the rotational isomeric state (RIS) approach^{3,4}. For each backbone bond, the continuous distribution of possible torsional angles is replaced by a finite number of values, corresponding to minima in the conformational energy curve, which are defined as rotational isomeric states. The chain is then represented as an equilibrium mixture of such states, each of which is characterized both by its torsional angle value and by its probability of occurrence. In general, these probabilities will be conditional in nature, since the probability for a bond to be in a given isomeric state will depend upon the state associated with the bond's nearest neighbours. This is expressed through a conditional probabilities matrix $U_i = [u_{\zeta\eta}]_i$. In this matrix, states ζ for bond $i-1$ index the rows, whereas states η for bond i index the columns. (The index i in the matrix can be dropped if all bonds are equivalent.) Each element $u_{\zeta\eta}$ represents the probability associated with bond i being in rotation state η , assuming that bond $i-1$ is in state ζ . In addition, $u_{\zeta\eta}$ will be related to the conformational energy difference $\Delta E_{\zeta\eta} = E_\eta - E_\zeta$.

Therefore, our model chain is randomly built, following the PTFE structure drawn in Figure 1. We assign values

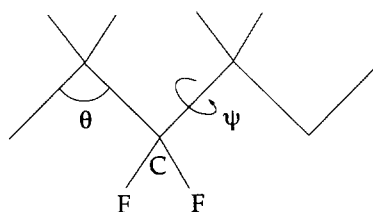


Figure 1 Schematic representation of a PTFE chain segment

for the relevant geometric parameters of the chain, i.e. bond lengths and backbone valence angle θ ; we then choose the finite number of backbone *trans* and *gauche* states appropriate for PTFE, the values for the corresponding torsional angles ψ and the conditional probabilities matrix associated with them. Torsional angles are defined such that a *trans* conformation corresponds to a 0° angle.

Finally, we can take into account temperature-induced variations in the torsional angles by introducing Gaussian distributions in the values of the backbone rotation angles.

Having created the chain, interatomic distances are calculated and a neutron diffraction pattern is obtained by applying the Debye relationship^{15,17,18}:

$$S_C(Q) = \frac{1}{N} \sum_i \sum_{j \neq i} b_i b_j \frac{\sin(Qr_{ij})}{Qr_{ij}}$$

where N is the number of atoms, b_i and b_j are the neutron scattering lengths associated with distinct atoms i and j ¹⁹ and r_{ij} is the distance between these two atoms.

In order to avoid the inclusion of near-neighbour distances that are effectively interchain in nature, due to the coiling of the chain on itself, the scattering can be calculated only for those atom pairs that are separated by less than a given number of bonds. An acceptable maximum number of skeletal bonds is usually 20¹⁸. This strategy has also the beneficial side effect of reducing computation time.

Furthermore, the model diffraction pattern was smeared with a Gaussian distribution of width proportional to Q , the proportionality factor being 0.03. This takes into account the finite experimental resolution, which on the diffractometer used is $\Delta Q/Q = 3\%$, as will be mentioned later.

In order to obtain a reasonable statistical model, the average of a number of chains is required. An equivalent approach is to calculate the scattering from a long chain, which also reduces any end effects. Since we were unable to construct a chain of equivalent length to the one characterizing the material being probed experimentally, we have studied the effects of both chain length and averaging over a number of chains on the accuracy and reliability of the model.

The structure factor $S_C(Q)$, calculated from the model chain, is then quantitatively compared to the experimental pattern $S_E(Q)$ via the following χ^2 test:

$$\chi^2 = \frac{1}{n_Q} \sum_{i=1}^{n_Q} [Q_i S_C(Q_i) - Q_i S_E(Q_i)]^2$$

where n_Q is the number of Q points in the scattering curve.

The comparison is performed on the Q -weighted structure factors in order to enhance the high- Q scattering region. Obviously, this comparison takes place over that portion of the scattering pattern containing no appreciable contributions from interchain correlations, namely over Q values higher than $\sim 2 \text{ \AA}^{-1}$.

Several models can be built by varying the different parameters defining the simulated chain. The χ^2 corresponding to each generated chain will then measure the accuracy of the model in describing the conformational correlations in the real polymer chain. The most accurate model will simply be the one corresponding to the minimum χ^2 value obtained. The strategy that we follow is the systematic variation of one model parameter at a

time, in a given range of possible values and with a given scan step size. This search strategy in the parameters space is essentially equivalent to the Ravine method²⁰. For any given parameter, the variability interval is wide at first and the scan step is rather large. The region of minimum χ^2 in the parameter space is then identified and the scan is repeated over a narrower interval with a smaller step. The procedure is repeated until the scan step corresponds to the desired accuracy for the given parameter. This procedure allows us to obtain information which is twofold in nature: on the one hand, the effect of that particular parameter on the overall structure factor can be studied, while on the other hand it is possible to adjust the single chain model of the polymer to 'fit' the experimental results. Once a minimum value for χ^2 has been obtained from the variation of one parameter, the corresponding value for that parameter is set in the model and a different parameter is explored. After all of the conformational parameters have been varied in turn, the procedure is repeated as many times as it is necessary to obtain a stable χ^2 value.

From the results of this 'refinement' technique, a picture of the polymer chain may be obtained. In particular, its flexibility can be determined by the probability of *trans* torsions that are obtained. The energy difference between *trans* and *gauche* states can be determined and the average of the straight sequence length can be estimated. Another important determinable parameter is the anisotropy of this straight sequence of chain segment, which can be obtained as an aspect ratio a , i.e. the ratio of length to diameter of the sequence. If the diameter of the straight conformation is d , a can be approximated directly from the first-order probabilities:

$$a = \frac{l}{d} \left(\frac{p_T + 1}{1 - p_T} \right) \quad (1)$$

where l is the projected skeletal bond length.

While being rather crude, this representation is particularly useful in providing a simple picture of the chain and in giving an insight into the possible types of packing arrangements.

SEMIEMPIRICAL QUANTUM MECHANICAL ORBITAL CALCULATIONS

In recent years a great interest has been demonstrated in the use of force field and molecular orbital calculations to predict polymer properties. In order to test this approach, we performed calculations using the semi-empirical molecular orbital program MOPAC²¹ and compared the results obtained via this route with the ones experimentally derived with the method described in the previous section.

MOPAC can be efficiently used to calculate polymer properties by taking advantage of the so-called cluster approach^{22,23}. Conventionally, polymers have been studied using solid-state methods such as tight-binding theory. In this approach, a Brillouin zone is constructed and sampled using a regular mesh of points. This produces a number of complex electron density matrices, from which the real density matrix can be derived.

The MOPAC approach is quite different: instead of sampling the whole Brillouin zone, only a single point is considered. The use of a single point requires the unit cell or repeat distance to be large enough for the

associated Brillouin zone to be so small that all bands are essentially flat. In other words, the repeat distance needs to be greater than 10 Å. A practical way to establish how large the repeat distance should be for a given polymer is to calculate the heat of formation on clusters characterized by an increasing number of repeat units. The heat of formation per repeat unit is expected to decrease at first with the increasing size of the cluster, but to converge subsequently towards a constant value. The speed of such a convergence, i.e. the required repeat distance length, depends on the degree of delocalization of the polymer structure.

This cluster model allows polymer calculations to be carried out with little more difficulty than that encountered in a similar calculation on molecules and ions. Furthermore, since the repeat unit's dimensions are normally rather large, the cluster can be frequently built up with just a few units.

The different calculation methods within MOPAC (MNDO, MINDO/3, AM1 and PM3) have many features in common. They are all self-consistent field (SCF) methods, they take into account electrostatic repulsion and exchange stabilization, and all calculated integrals in them are evaluated by approximate means. Furthermore, they all use a restricted basis set of one s orbital and three p orbitals per atom and ignore overlap integrals in the secular equation. All four semiempirical methods contain sets of parameters, but not all elements are parameterized for all methods.

We have been using the computational program to perform complete geometry optimizations with the different available Hamiltonians. Geometry optimization is an energy minimization technique that proceeds by calculating the resultant forces on each atom in the system (using the derivatives of the energy with respect to coordinates) and then moving the atoms in the direction determined by these factors so as to lower the energy of the system. When the geometry is within a preset distance or energy of a local minimum, the optimization is stopped. MOPAC does not necessarily converge to the global minimum for the system. The optimized geometry will correspond to an isomer or conformer, with the degree of optimization being specified by the user.

We have also tested the sensitivity of the computational technique to geometric parameters such as bond lengths or backbone valence angles. The procedure is based on an analysis of the evolution of the molecule's heat of formation as one geometric parameter is varied systematically over a range of values. This allows us to determine the role of the variable geometric parameter in the modelling Hamiltonian, plus the size of the fluctuations of this parameter which will be present in the material. Obviously, the best value for this parameter, corresponding to a minimum in the heat of formation curve, will have to match the results obtained in the geometry optimization calculation.

EXPERIMENTAL

The material used was commercial PTFE (ICI Fluon), in the form of a 7 mm diameter cylindrical rod, with the sample being contained in a vanadium cylindrical can.

The measurements were performed on the Liquid and Amorphous time-of-flight Diffractometer (LAD) at the

pulsed neutron source, ISIS (Chilton, UK)²⁴. The vanadium can was mounted on the standard furnace of the diffractometer. We carried out measurements at two different temperatures in the melt, namely 350 and 400°C, i.e. just above the melting transition temperature and just before the high-temperature degeneration of the material, respectively: the stability of the material at 400°C had been previously tested. The temperature inside the furnace was stable within 0.5°C, and the duration of each run was ~10 h.

For each one of the 16 detector banks, the raw data were normalized for the incident beam flux and calibrated with a standard cylindrical vanadium sample. Corrections were made for absorption, multiple scattering and self-scattering contributions. Data from the different detector banks were finally merged and the total structure factor $S(Q)$ was obtained. This data reduction was performed with the ATLAS suite of programs, available at ISIS for the analysis of time-of-flight diffraction data²⁴. The data thus obtained were characterized by a constant $\Delta Q/Q$ resolution²⁵.

RESULTS AND DISCUSSION

Figure 2 shows the experimental static structure factor $S(Q)$ of molten PTFE at a temperature of 350°C as a function of the exchanged momentum Q , after data correction and normalization. After the first, dominant peak, which is interchain in nature, the two main features are a peak at $\sim 3 \text{ \AA}^{-1}$, which arises mainly from F-F interactions and a peak at $\sim 5 \text{ \AA}^{-1}$, indicating correlations between carbon atoms along the chain. The triangular nature of the first intrachain peak has been previously shown to indicate the presence of long segments in a *trans*-type conformation¹². The Q -weighted scattering pattern was then calculated and the region between 2.5 and 35 Å^{-1} was used as a quantitative comparison with the scattering function predicted by the various models.

The model was a PTFE chain consisting of 5000 skeletal bonds. The chain was built with four isomeric states, i.e. a split *trans* state and two *gauche* states, according to previous conformational energy calculations²⁶, as well as an analysis of the experimental dipole moments in perfluoroalkane molecules⁹.

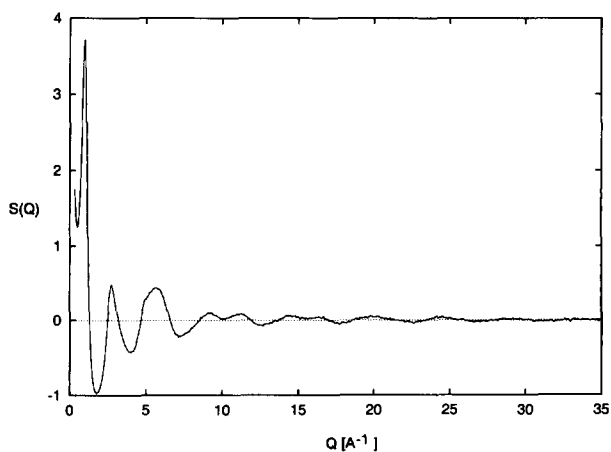


Figure 2 Experimental $S(Q)$ curve for PTFE at $T = 350^\circ\text{C}$, after data correction and normalization

The conditional probabilities associated with these isomeric states were represented by the following matrix:

$$\begin{pmatrix} (t^+) & (t^-) & (g^+) & (g^-) \\ \alpha\beta & \alpha(1-\beta) & 1-\alpha & 0 \\ \alpha(1-\beta) & \alpha\beta & 0 & 1-\alpha \\ \alpha & 0 & 1-\alpha & 0 \\ 0 & \alpha & 0 & 1-\alpha \end{pmatrix} \quad (2)$$

where α is the probability of a *trans* state and β is the probability of a given state preserving its sign. The varying parameters of the model were C-C and C-F bond lengths, backbone valence angle θ , backbone torsion angles corresponding to each one of the four isomers, i.e. ψ_t and ψ_g for the two *trans* and *gauche* states respectively, forced to vary coupled (i.e. $\psi_{t,-} = -\psi_{t,+}$), and α and β in the probability matrix. The bond lengths and bond angles were characterized by the same values throughout the chain.

The initial values for the parameters were taken from the literature. They were 1.54 and 1.36 Å for the bond lengths, 114° for the θ angle, $\pm 15^\circ$ and $\pm 120^\circ$ for the torsional angles, 0.84 for α and 0.76 for β . Figure 3 shows the corresponding neutron scattering pattern and its comparison with the experimental results. As can be seen, the main features in the experimental curve are represented by the model curve, but the peak positions and relative intensities are not quantitatively predicted.

The 'refinement' procedure was then started. For each model parameter, an initial scan interval and a scan step were chosen. Several models were built, in which the parameter of interest was set to one of the scan values, while the other parameters were frozen to their initial values. The expected diffraction patterns were calculated for every model and the corresponding χ^2 values evaluated. The region of minimum χ^2 in the parameter space was then identified and the span was refined over a narrower interval with a smaller scan step. The procedure was repeated until the scan step corresponded to the desired accuracy for the given parameter. The best value for the parameter of interest was obtained from the minimum in the χ^2 curve. The refinement procedure was then repeated for a different parameter, after having fixed the previous parameter to the best value found. The

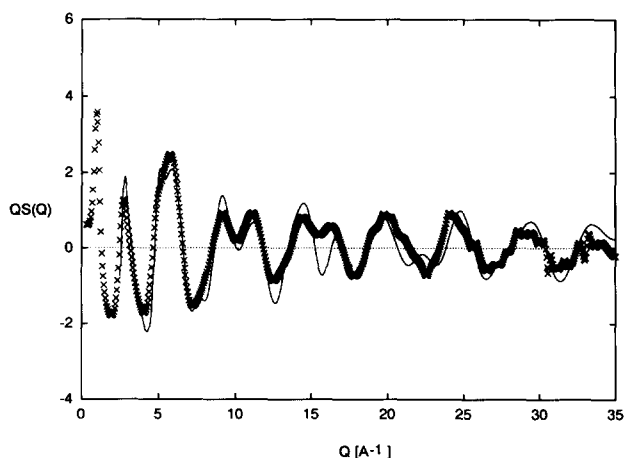


Figure 3 Comparison of model prediction (continuous line) with experimental neutron diffraction data at $T=350^\circ\text{C}$ (+), using the model parameters reported in the literature

overall procedure was finally repeated as many times as was necessary to achieve convergence of the χ^2 .

It is to be noted that, for each parameter, the model scattering pattern was calculated as an average of the scattering patterns obtained by a number of equivalent models. The number of models over which the average was performed depended upon the accuracy required for the particular parameter under investigation. For example, while a single model was sufficient to determine bond lengths to an accuracy of 0.01 Å, an average over 20 analogous models was necessary to discriminate between two neighbouring values for α or β , within 0.01. Figures 4 and 5 show examples of the tests performed to this aim. Figure 4a represents χ^2 curves obtained by varying the parameter β and averaging over a variable number of models, with a chain consisting of 1000 skeletal bonds. Figure 4b shows the same calculation with a model chain of 5000 bonds. As can be expected, the shorter-chain model needs an averaging over 50 models to obtain a reasonably smoothly varying curve, whereas the 5000-bonds chain model only requires an average over 10 analogous models, with a resulting saving in computation time. Figure 5 represents the standard deviation σ of the distribution of χ^2 values for 10 independent χ^2 calculations from a given model,

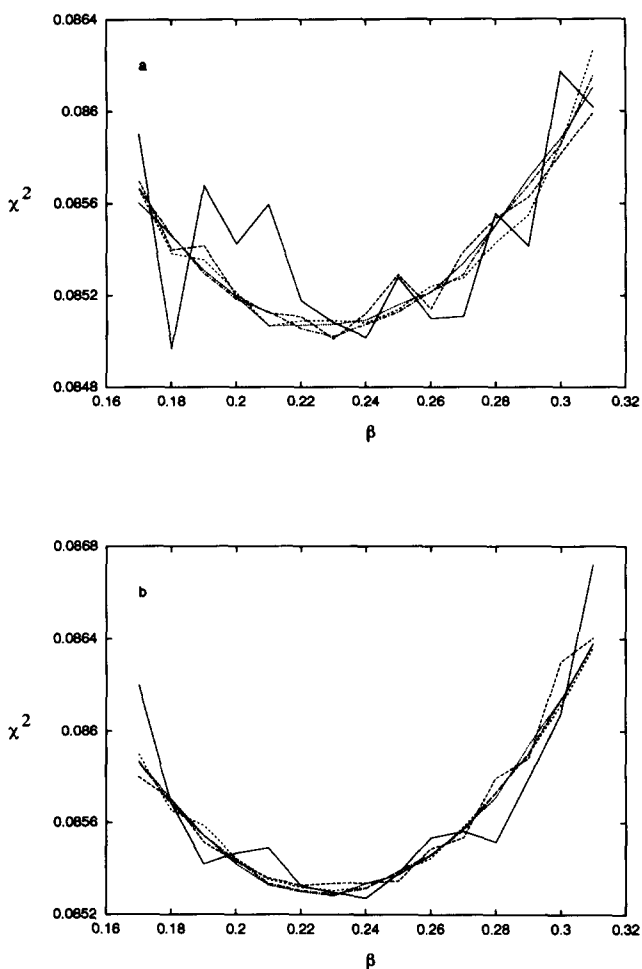


Figure 4 Representative behaviour of χ^2 as a function of the probability parameter β for (a) a 1000-bonds chain and (b) a 5000-bonds chain. The different curves represent averaging of the calculated scattering pattern over a number of equivalent models: (continuous line) 1; (long dashed line) 10; (short dashed line) 20; (dotted line) 50; (dashed-dotted line) 100 models

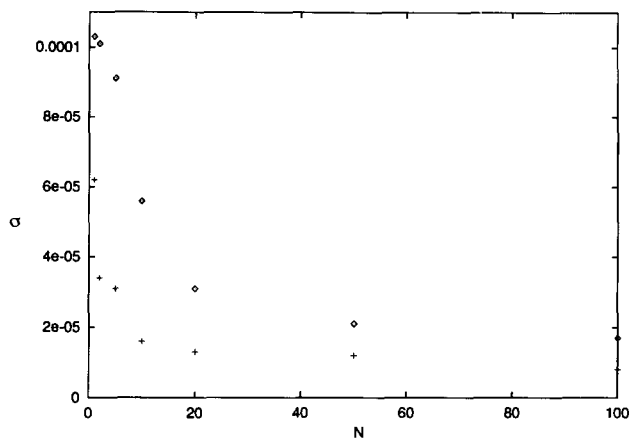


Figure 5 The standard deviation σ of χ^2 for 10 equivalent models as a function of the number of models N in the averaging procedure: (\diamond) a 1000-bonds chain; (+) a 5000-bonds chain

corresponding to different numbers N of averages for the two chain lengths of 1000 and 5000 bonds. Once again, σ can be seen to reach rapid saturation at an average over a number of models equal to 10 for the longer chain. As a result of these tests, all our models were built using a 5000-skeletal-bonds chain and an averaging over 1, 10 and 20 models for bond lengths, bond angles and conditional probability parameters, respectively.

Figure 6 shows typical χ^2 curves obtained from final scans of the geometric parameters, i.e. bond lengths, θ valence angle and *trans* and *gauche* torsional angles. The experimental data from which the χ^2 values of Figure 6 were calculated are obtained at $T=350^\circ\text{C}$. For each curve, the value of the parameter corresponding to the minimum in χ^2 was obtained by direct examination of the curve, rather than through interpolation of the curve

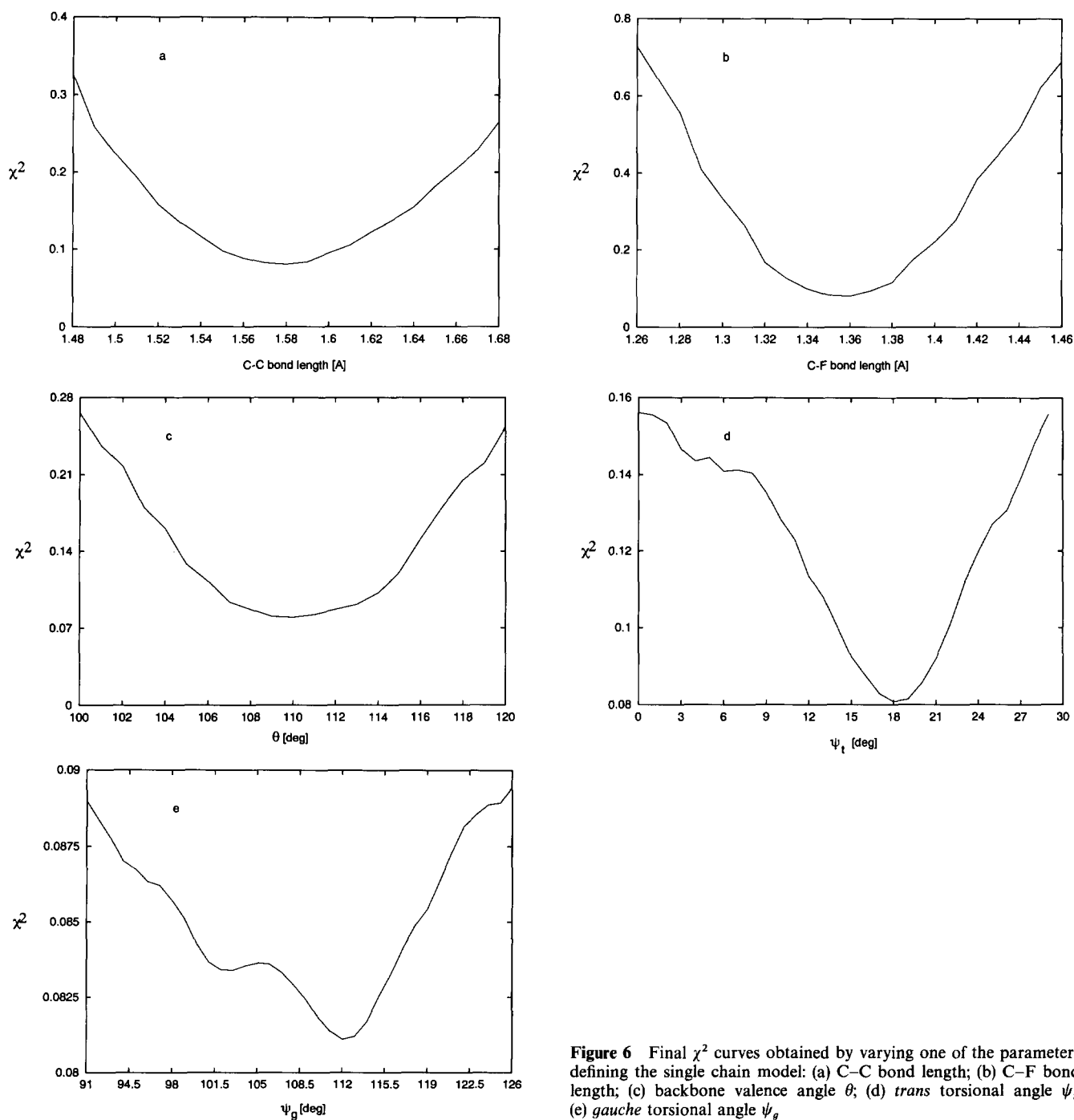


Figure 6 Final χ^2 curves obtained by varying one of the parameters defining the single chain model: (a) C-C bond length; (b) C-F bond length; (c) backbone valence angle θ ; (d) *trans* torsional angle ψ_t ; (e) *gauche* torsional angle ψ_g

itself. In other words, the 'best-fit' value for any given parameter was one of the points scanned during the search. The precision of this value was determined by the resolution chosen in the grid-scan procedure. From the curves of Figure 6 we obtained the following values for the geometric parameters: 1.58 and 1.36 Å for the C–C and C–F bond lengths, respectively (Figures 6a and 6b, respectively), 110° for the θ valence angle (Figure 6c) and $\pm 18^\circ$ and $\pm 112^\circ$ for the two *trans* and *gauche* torsional angles, respectively (Figures 6d and 6e, respectively). The existence of a split *trans* state is confirmed by the fact that a three-rotational-states model does not produce a satisfactory fit to the experimental data, as is shown in Figure 6d. This agrees with a previously suggested model^{5,9}. The value of the angle, corresponding to the helical deformation which is found, is in agreement with all of the theoretical predictions presented in the literature^{26–34}. Similar values for the C–C and C–F bond lengths were obtained by inspection of the corresponding radial distribution function that was obtained by Fourier transformation of the data shown in Figure 2.

As regards the conditional probabilities, since the two probability parameters α and β are interdependent, a grid-search strategy was applied: having roughly localized the region between 0.8 and 1.0 as that containing the best α value (with β arbitrary), α was fixed at a starting value and a χ^2 curve was obtained by varying β . The value for α was then changed and a new χ^2 curve was calculated. The procedure was repeated with α being set to values in the range 0.8–1.0. Each χ^2 curve that was obtained was analysed and the β value giving the minimum χ^2 , at the corresponding set value of α , was recorded. All of the minimum χ^2 values obtained from the several curves were finally compared with each other, and the absolute minimum value was then selected. The α , β couple corresponding to this absolute minimum was thus chosen as defining the best probability parameters for the model chain. In this way, we obtained the values $\alpha=0.86$ and $\beta=0.25$ at $T=350^\circ\text{C}$. The probability of *trans* (i.e. α) obtained is in very good agreement with the results predicted at 600 K by the analysis of dipole moments in perfluoroalkanes (obtained with the assumption that the energy barriers are for *trans/gauche* transitions^{9,35}). The resulting probability of the torsions being *trans* corresponds to straight chain sequences of ~ 25 Å and to an aspect ratio of 3.2. This is in agreement with previous conclusions from X-ray measurements¹³. As pointed out in the literature¹², this would suggest a high degree of orientational correlations between chain segments. By assuming that the correlation extends in a spherical diameter equal to the persistence length, it has been shown¹³ that an aspect ratio of ~ 3 implies a sphere including nearest neighbours (while a higher aspect ratio, i.e. a higher probability of *trans*, would allow the inclusion of second and third nearest neighbours). Thus, a correlation sphere of 15 Å in radius might be expected for PTFE. The possibility of a high level of orientational correlations in PTFE has been theoretically predicted in previous work³⁶, in which it was shown that the chains characteristic of PTFE are at the boundary of liquid crystal formation. Optically, PTFE melts are isotropic and hence they do not form liquid crystalline phases. The aspect ratio of 3 therefore sets a lower limit for the formation of liquid crystal phases in simple main-chain systems.

The value obtained for β implies a high rate of helix

reversals, as was previously suggested^{5,13}. A considerable level of helix reversals has been deemed responsible for the intrachain disorder observed in the crystalline state in relatively recent X-ray investigations^{37,38}.

Figure 7 shows the projected trajectory of a portion of the best model chain. As can be seen, the chain configuration is characterized by considerably long all-*trans* sequences.

Having obtained the best model, we also considered the possibility of temperature-induced oscillations in the values of the torsional angles around the minimum of their potential well. This was achieved by introducing a standard deviation ϕ_{tosc} for the distributions of torsional angles, which was assumed Gaussian. The standard deviation ϕ_{tosc} was varied and the value of χ^2 was evaluated. The fit to the experimental diffraction pattern is only marginally improved by this parameter, as was previously concluded from the analysis of X-ray data¹³. The best value found for ϕ_{tosc} was 5° at $T=350^\circ\text{C}$.

Figure 8 shows the predicted Q -weighted scattering function for the model that corresponds to the minimum χ^2 , at $T=350^\circ\text{C}$. As can be seen, the agreement between the model and the experimental results is good, over the whole of the Q range considered (between 2.5 and 35 \AA^{-1}).

Table 1 summarizes the values found for the various structural parameters at two different temperatures, namely 350 and 400°C . At the higher temperature, the

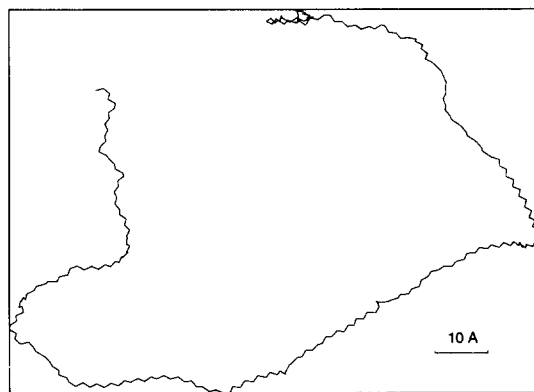


Figure 7 Typical chain trajectory; note the extended all-*trans* sequences

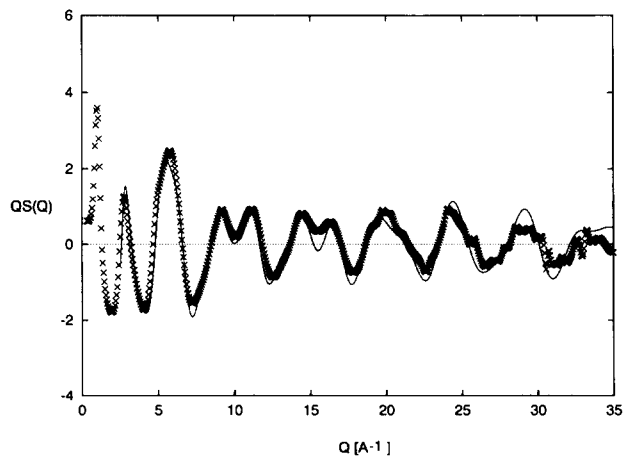


Figure 8 Best fit to the experimental diffraction pattern of molten PTFE at 350°C , over the Q range $2.5\text{--}35 \text{ \AA}^{-1}$; (continuous line) model predicted values; (+) experimental data

Table 1 Configurational parameters of the single chain model corresponding to minimum χ^2 at two different temperatures in the melt. Calculations performed over the Q range from 2.5–35 Å⁻¹

T (°C)	C–C (Å)	C–F (Å)	θ (deg)	ψ_t (deg)	ψ_g (deg)	α	β	ϕ_{tosc} (deg)
350	1.58 ± 0.01	1.36 ± 0.01	110 ± 1	± 18.0 ± 0.5	± 112 ± 1	0.86 ± 0.01	0.25 ± 0.02	5 ± 2
400	1.58 ± 0.01	1.36 ± 0.01	110 ± 1	± 18.0 ± 0.5	± 112 ± 1	0.84 ± 0.01	0.24 ± 0.02	5 ± 2

quality of the fit that is obtained is comparable to the one determined at 350°C. An observation of the same values for bond lengths and valence angles is encouraging. On the other hand, the 0.02 difference in the probability of *trans/gauche* transitions with variation in temperature coincides with the variation that would be expected from the relationship

$$p_{tg} = \exp\left(-\frac{E_{tg}}{RT}\right)$$

where E_{tg} , obtained from the probabilities parameters derived from the fit at $T=350^\circ\text{C}$, is 6.7 kJ mol⁻¹ (1.6 kcal mol⁻¹) and is assumed to be temperature-independent (the validity of this assumption was demonstrated by Bates and Stockmayer^{9,35}).

We have used in this work a comparison between the Q -weighted structure factors obtained from experiment and by calculation from each model. Calculations using a weighting of Q^n , with $n=0, 1, 2$, all yielded similar results although the level of uncertainty associated with each result varied. Geometric factors, such as the bond lengths, have a marked imprint on the structure factors, especially at high values of Q , and hence it is relatively straightforward to extract such parameters. In contrast, the influence of the nature of the distribution of the rotation states along the polymer chain on the structure factor is not so strong and is more marked at lower values of Q . Hence, for example, evaluation of these parameters using a Q^2 weighting results in an increased uncertainty with respect to the values of α and β although the minimum values found in the χ^2 curves were similar for all weightings. Therefore, weighting with Q provided a reasonable balance between the opposing factors involved in the evaluation of the wide range of conformational parameters studied in this work.

The values derived for the geometric parameters from the experimental diffraction pattern may be used to critically examine the results that we obtained from the semiempirical MOPAC calculations. In the MOPAC analysis, we started from all-*trans* chain segments. We calculated at first the heat of formation associated with polymer clusters characterized by an increasing number of repeat units. After a progressive decrease for small clusters, the heat of formation per repeat unit stabilized to a constant value for clusters of 10–14 CF₂ units. Therefore, we chose a 12 CF₂ units segment in all of the ensuing calculations. Table 2 shows the results of geometry optimizations performed with the different available Hamiltonians. The required precision in all calculations was 100 times higher than the default precision, with the default criterion ensuring a heat of formation within less than 0.4 J of the correct semiempirical answer. The MNDO method predicts a heat of formation per CF₂ unit that exactly matches the results reported from analogous calculations by Stewart on a series of

Table 2 Summary of results obtained in this work from MOPAC calculations

C–C (Å)	C–F (Å)	θ (deg)	ψ_t (deg)	H_f^a (kJ mol ⁻¹)	Method
1.67	1.34	113	0	-353.84	MNDO
1.61	1.37	109	0	-377.56	AM1
1.61	1.35	111	0	-445.89	PM3, no cluster ^b
1.61	1.35	111	± 16	-401.70	PM3-DFP ^c
1.60	1.35	110	± 18	-403.33	PM3-BFGS ^d

^a Calculated heat of formation per CF₂ unit

^b Calculation performed on an all-*trans* C₁₂F₂₄ molecule

^c David-Fletcher-Powell (DFP) minimization algorithm³⁹

^d Broyden-Fletcher-Goldfarb-Shanno (BFGS) minimization algorithm⁴⁰

polymers, including PTFE²³. The geometric parameters listed in Table 2 have values that are close to the results obtained by the independent experiment/ χ^2 modelling approach, for calculation methods other than MNDO, which predicts a considerably larger C–C bond length. In particular, both approaches predict a lengthening of the C–C bond length with respect to the ideal value of 1.54 Å for an isolated bond, which is to be attributed to the strong repulsion of the fluorine atoms. It is to be noted though that the MOPAC predicted C–C bond length is always larger than the experimental evidence.

Furthermore, the *trans* torsional angle values listed in Table 2 are very interesting to consider. Of all of the available methods, only the most recent, namely PM3, predicts a helical distortion of the all-*trans* configuration, the distortion angle being 18°, in agreement with all of the previous evidence. This helicity is only predicted on a cluster-like periodic structure, not on the corresponding isolated molecule. These results lead to two conclusions. First, the periodicity of the cluster structure is fundamental in determining the observed helical conformation of PTFE. Secondly, the reason for the accuracy of only the PM3 Hamiltonian in dealing with this particular polymer is probably to be found in the fact that, of all the MOPAC methods, PM3 is the only one for which the parameters referring to s and p atomic orbital repulsion integrals have been optimized²¹.

The optimized geometry obtained with the PM3 calculation was then used to perform reaction coordinate scans to determine the values of bond lengths and backbone valence angle giving rise to the lowest heat of formation. For each parameter explored, the resolution in the reaction coordinate space was set at the same value as the step ultimately chosen in the scattering refinement procedure. The calculations were performed both with and without geometry optimization for each intermediate structure generated in the scan procedure. Figure 9 shows typical reaction coordinate curves, both

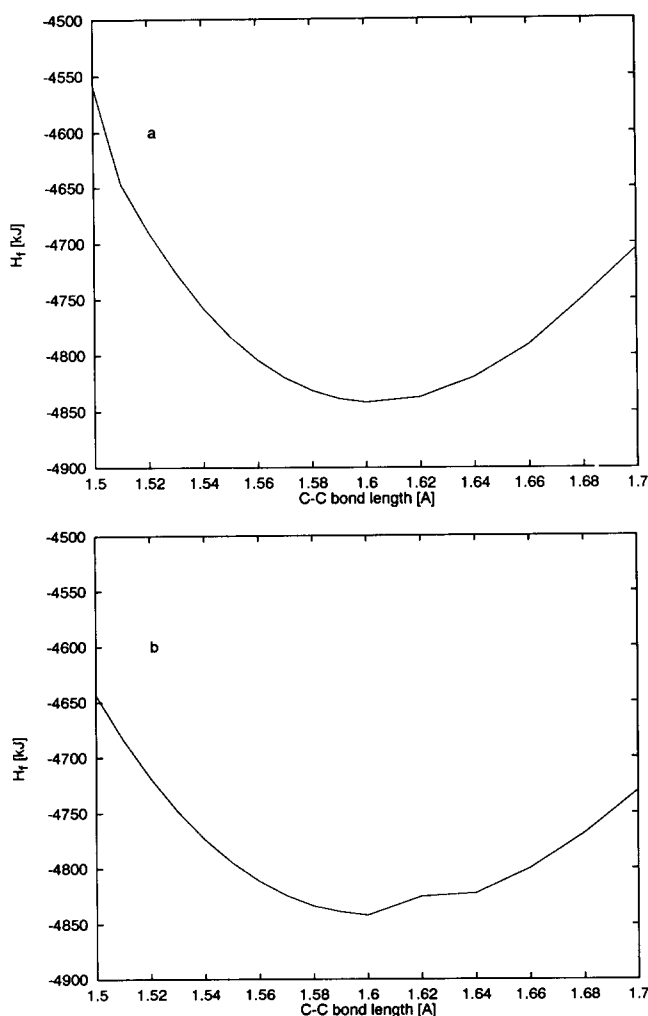


Figure 9 Typical heat of formation curves obtained in a MOPAC reaction coordinate calculation, with the reaction coordinate in this case being the C-C bond length: (a) no energy optimization; (b) energy optimization of each intermediate structure

without (Figure 9a) and with (Figure 9b) geometry optimization at each point in the curve. As can be seen, the range of variability of the heat of formation changes in the two cases, but the position of the minimum of the curve is left unchanged. The best values for the geometric parameters obtained from this procedure confirm the values predicted by the geometry optimization, i.e. C-C = 1.60 Å, C-F = 1.35 Å and $\theta = 110^\circ$.

A comparison with theoretical predictions of the conformation of the PTFE chain that are present in the literature is not very straightforward, due to the large number of often contrasting data presented. Table 3 summarizes results previously obtained by using several different force fields. As can be seen, there is no general agreement either on the position of the *gauche* minima in the torsional energy curve or on the relative depth of such minima. This is due to the difference in the ingredients chosen by the various authors to describe the torsional potential. This is particularly crucial in a polymer such as PTFE, where non-bonded interactions are rather delicate and difficult to account for. It is to be noted that these works present a smaller value for the C-C bond length than that determined by experiment in this work. In most of the cases, this parameter was not obtained from the calculations, but assigned at the start as an input parameter. Furthermore, the reported values for the θ valence angle are all substantially higher than the one found by us in this work. On the contrary, the C-F bond length is variable over an interval which is reasonably centred around the values found by us.

Finally, we applied the same fit strategy to a smaller portion of the experimental diffraction pattern, i.e. $2.5\text{--}10\text{ \AA}^{-1}$; this is the Q range that would normally be explored by X-ray experiments. The resulting model parameters are summarized in Table 4. While the quality of the fit is satisfactory, the model converges, as the table indicates, to a slightly different configuration for the PTFE chain. We believe that this is an indication of the

Table 3 Comparison of values obtained for the geometric parameters in this work with literature data

C-C (Å)	C-F (Å)	θ (deg)	ψ_t (deg)	ψ_g (deg)	E_t^a (kJ mol ⁻¹)	$E_t - E_g^b$ (kJ mol ⁻¹)	Ref.
1.543	1.330		± 14				27 ^c
1.54	1.36	114.30	± 17.30		-1.7		28 ^c
1.54	1.38	116	± 15	$\pm 90, \pm 120$	-1.2	4.2, 25	29 ^d
1.54	1.41	109.28-116	± 17	$\pm 87, \pm 120$	-7.5	8, 418	26 ^{d,e}
1.53	1.36	114	± 17	± 120	-2.22	8.4	30
1.54	1.36	114.6	$\pm 10, \pm 15$	$\pm 120, \pm 90$	-2.9		31 ^d
1.52	1.31	112	± 5		-19.2		32 ^c
1.54	1.36	114.4	± 15	$\pm 90, \pm 120$	-7.9	10.0, 40.2	33 ^d
1.54	1.36	114.6	± 15	$\pm 90, \pm 120$	-5.0	10.0, 22.6	34 ^d

^a Value of the energy per CF₂ unit at the bottom of the *trans* wells

^b $E_t - E_g$ is the energy difference between *trans* and *gauche* minima

^c *Gauche* isomers not calculated

^d The two different *gauche* isomers are listed in order of decreasing energy well depth

^e Calculations performed with both values of the θ angle; results do not differ greatly

Table 4 Configurational parameters of the single chain model corresponding to minimum χ^2 for two different Q ranges; both calculations performed on the data at $T = 350^\circ\text{C}$

Q range (Å ⁻¹)	C-C (Å)	C-F (Å)	θ (deg)	ψ_t (deg)	ψ_g (deg)	α	β	ϕ_{isoc} (deg)
2.5-35.0	1.58 ± 0.01	1.36 ± 0.01	110 ± 1	$\pm 18.0 \pm 0.5$	$\pm 112 \pm 1$	0.86 ± 0.01	0.25 ± 0.02	5 ± 2
2.5-10.0	1.60 ± 0.01	1.36 ± 0.01	112 ± 1	$\pm 18.0 \pm 0.5$	$\pm 115 \pm 1$	0.90 ± 0.01	0.28 ± 0.02	4 ± 2

importance of including the information present in the high- Q diffraction pattern to obtain a really quantitative description of the intrachain order.

CONCLUSIONS

In this study we have demonstrated the possibility of carrying out a detailed quantitative analysis of the single chain conformation of a non-crystalline polymeric material through the combination of neutron scattering over a wide Q range and a modelling technique rather similar to the procedure known as 'structure refinement' in crystalline materials.

We have shown the high sensitivity of neutron diffraction to the details of intrachain correlations and the capability of a relatively simple and straightforward statistical model to reproduce an amorphous diffraction pattern with reasonable accuracy, once the Q region characterized by interchain correlations is excluded from the analysis. The fit of the model to the experimental data can give useful information, not only on the chemical features of the polymer repeat unit, which are to a large extent known a priori, but also, and most importantly, on the degree of stiffness of the polymer chain and on its anisotropy.

The method has given satisfactory results for molten PTFE, thus providing a single chain model in which the C-C and C-F bond lengths are 1.58 and 1.36 Å, respectively, the backbone valence angle is 110° and the four isomers describing the torsional potential are at angles of $\pm 18^\circ$ for the *trans* conformers and $\pm 112^\circ$ for the two *gauche* states. The splitting of the *trans* state is responsible for a helical distortion of the chain. The probability of *trans* conformers is 0.86 at $T = 350^\circ\text{C}$ and decreases slightly to 0.84 at $T = 400^\circ\text{C}$. This high fraction of *trans* conformers produces a stiff chain, characterized by long all-*trans* sequences, which are also rather anisotropic, with the evaluated aspect ratio being 3.2. This anisotropy may imply the existence of considerable local interchain orientational correlations.

Finally, we have used the experimental results obtained to establish the viability of semiempirical molecular orbital methods for this unusual polymer. We have shown the importance of the choice of Hamiltonian for the description of the system. Of all the available methods within MOPAC, only the PM3 method predicts, in fact, the distortion of an otherwise planar all-*trans* chain into a helical structure, as observed experimentally. We have also shown the convergence of the MOPAC geometry optimization procedures to geometric parameters for the chain that are largely in agreement with the ones that have been determined experimentally.

ACKNOWLEDGEMENTS

This work forms part of the Courtaulds Polymer Science Prize Programme at the University of Reading. It was

also supported by the Science and Engineering Research Council. We also acknowledge the support of Polygen Corporation (now Molecular Simulation Inc.).

REFERENCES

- Mitchell, G. R. in 'Order in the Amorphous "State" of Polymers' (Eds S. E. Keinath, R. L. Miller and J. K. Rieke), Plenum, New York, 1987, p. 1
- Mitchell, G. R. in 'Comprehensive Polymer Science' (Eds G. Allen, J. C. Bevington, C. Booth and C. Price), Vol. 1, Pergamon, Oxford, 1989, Ch. 31, p. 687
- Flory, P. J. 'Statistical Mechanics of Chain Molecules', Wiley, New York, 1969
- Volkenstein, M. V. 'Configurational Statistics of Polymeric Chains', Wiley, New York, 1963
- Bates, T. W. in 'Fluoropolymers' (Ed. L. A. Wall), Wiley, New York, 1972, Ch. 14, p. 451
- Bunn, C. W. and Howells, E. R. *Nature (London)* 1954, **174**, 549
- Bunn, C. W. *Trans. Faraday Soc.* 1939, **35**, 482
- Scott, R. A. and Scheraga, H. A. *J. Chem. Phys.* 1965, **42**, 2209
- Bates, T. W. and Stockmayer, W. H. *Macromolecules* 1968, **1**, 12
- Tonelli, A. E. *Macromolecules* 1980, **13**, 734
- Kilian, H. G. and Jenckel, E. *Z. Elektrochem.-Angew. Phys. Chem.* 1959, **63**, 308
- Lovell, R., Mitchell, G. R. and Windle, A. H. *Faraday Discuss. Chem. Soc.* 1979, **68**, 46
- Mitchell, G. R. *PhD Thesis* CNA, 1983
- Mitchell, G. R. and Rosi-Schwartz, B. *Physica B* 1992, **180-181**, 558
- Mitchell, G. R. Technical Report 03/86, J.J. Thomson Physical Laboratory, University of Reading, 1986
- Birshtein, T. M. and Pitisyn, O. B. 'Conformations of Macromolecules', Interscience, New York, 1966
- Warren, B. E. 'X-Ray Diffraction', Addison-Wesley, Reading, MA, 1969
- Mitchell, G. R., Lovell, R. and Windle, A. H. *Polymer* 1982, **23**, 1273
- Windsor, C. G. 'Pulsed Neutron Scattering', Taylor and Francis, London, 1981
- Bevington, P. R. 'Data Reduction and Error Analysis for the Physical Sciences', McGraw-Hill, New York, 1969
- Stewart, J. J. P. *J. Comput. Aided Mol. Design* 1990, **4**, 1
- Perkins, P. G. and Stewart, J. J. P. *J. Chem. Soc. Faraday Trans. 2* 1980, **76**, 520
- Stewart, J. J. P. *New Polym. Mater.* 1987, **1**, 53
- Howells, W. S., Soper, A. K. and Hannon, A. C. Technical Report RAL-89-046, Rutherford Appleton Laboratory, Chilton, 1989
- ISIS, Technical Report, Rutherford Appleton Laboratory, Chilton, 1992
- McMahon, P. E. and McCulloch, R. L. *Trans. Faraday Soc.* 1965, **61**, 197
- Mason, E. A. and Kreevoy, M. M. *J. Am. Chem. Soc.* 1955, **77**, 5808
- Iwasaki, M. *J. Polym. Sci. (A-1)* 1963, **1**, 1099
- De Santis, P., Giglio, E., Liguori, A. M. and Ripamonte, A. *J. Polym. Sci. (A-1)*, 1963, **1**, 1383
- Bates, T. W. *Trans. Faraday Soc.* 1967, **63**, 1825
- D'Ilario, L. and Giglio, E. *Acta Crystallogr. Sect B* 1974, **30**, 372
- Springborg, M. and Lev, M. *Phys. Rev. B* 1989, **40**, 3333
- Napolitano, R., Pucciariello, R. and Villani, V. *Makromol. Chem.* 1990, **191**, 2755
- Villani, V., Pucciariello, R. and Ajroldi, G. *J. Polym. Sci., Polym. Phys. Edn* 1991, **29**, 1255
- Bates, T. W. and Stockmayer, W. H. *Macromolecules* 1968, **1**, 17
- Ronca, G. and Yoon, D. Y. *J. Chem. Phys.* 1982, **76**, 3295
- Corradini, P., De Rosa, C., Guerra, G. and Petraccone, V. *Macromolecules* 1987, **20**, 3043
- De Rosa, C., Guerra, G., Petraccone, V., Centore, R. and Corradini, P. *Macromolecules* 1988, **21**, 1174
- Fletcher, R. and Powell, M. J. D. *Comput. J.* 1966, **10**, 406
- Shanno, D. F. *J. Optim. Theory Appl.* 1985, **46**, 87